Flow Measurement and Instrumentation 75 (2020) 101808

Contents lists available at ScienceDirect

Flow Measurement and Instrumentation

journal homepage: www.elsevier.com/locate/flowmeasinst

# Modeling of the flow comparator as calibration device for high pressure natural gas flow metering in Modelica

Sukhwinder Singh [a,*], Gerhard Schmitz [a], Bodo Mickan [b]

[a] Institute for Engineering Thermodynamics, Hamburg University of Technology, Germany
[b] Physikalisch-Technische Bundesanstalt, Braunschweig, Germany

A B S T R A C T

The German national metrological institute, Physikalisch-Technische Bundesanstalt, is developing a new concept a for a volumetric primary standard to calibrate high pressure gas flow meters. The TUHH is supporting these Research & Development activities with its competence to elaborate computational models for detailed analysis of complex electromechanical systems including fluid flow aspects. The new primary standard is called Flow Comparator and uses an actively driven piston prover to measure the gas flow rate using the time the piston needs to displace a defined enclosed volume of gas in a cylinder. A computational model is developed in Modelica® to investigate the Flow Comparator's dynamic behavior and interaction with other components in the loop. The validation of the developed model shows good compliance with measured piston velocity and differential pressure at the piston. The model is used to optimize the frequency inverter's control voltage trajectory to increase the available calibration time.

## 1. Introduction

Natural gas is one of the most frequently used energy carriers worldwide and is usually transported in high pressure pipelines or as liquefied natural gas in tank vessels. In regards to the trade with natural gas, the uncertainty of high-pressure natural gas flow meters is of major importance. The uncertainty depends on the calibration chain and increases with each step. At the top of the calibration chain in Germany is the primary standard for high pressure natural gas flow metering. It is a High-Pressure Piston Prover (HPPP), which is installed and operated at the calibration facility for gas meters pigsar™ in Dorsten, Germany [1–3]. The HPPP can be operated with an inlet pressure up to 90 bar and flow rates up to 480 $m^3/h$ [3].

Due to the increasing size and flow rates of the gas flow meters and the limited operation range of the current national standard, a new concept for calibrating gas flow meters is being developed, the so-called Flow Comparator (FC). In order to conduct preliminary tests and to investigate the controllability as well as the usable flow rate, a prototype under atmospheric conditions is used. The Flow Comparator prototype in a closed loop configuration is shown in Fig. 1.

**Fig. 1.** Picture of the Flow Comparator prototype in a closed loop configuration.

## 2. Experimental setup

A simplified scheme of the experimental setup is shown in Fig. 2. The two main components of the Flow Comparator are a piston within a cylinder. The cylinder has two layers, one with magnetic properties and the other one acts as an electrical conductor.

Furthermore, the piston has an integrated stator core with windings and together the piston and the cylinder act as an asynchronous linear induction motor (LIM). The electrical power for the LIM is supplied through a cable connected to the piston. The acting force on the piston is controlled by a frequency inverter whose voltage and frequency can be controlled. The piston has an integrated check valve to limit the pressure drop across the piston. A more detailed scheme of the piston is shown in Fig. 3.

* Corresponding author.
*E-mail address:* sukhwinder.singh@tuhh.de (S. Singh).

https://doi.org/10.1016/j.flowmeasinst.2020.101808
Received 12 December 2019; Received in revised form 7 May 2020; Accepted 9 August 2020
Available online 29 August 2020

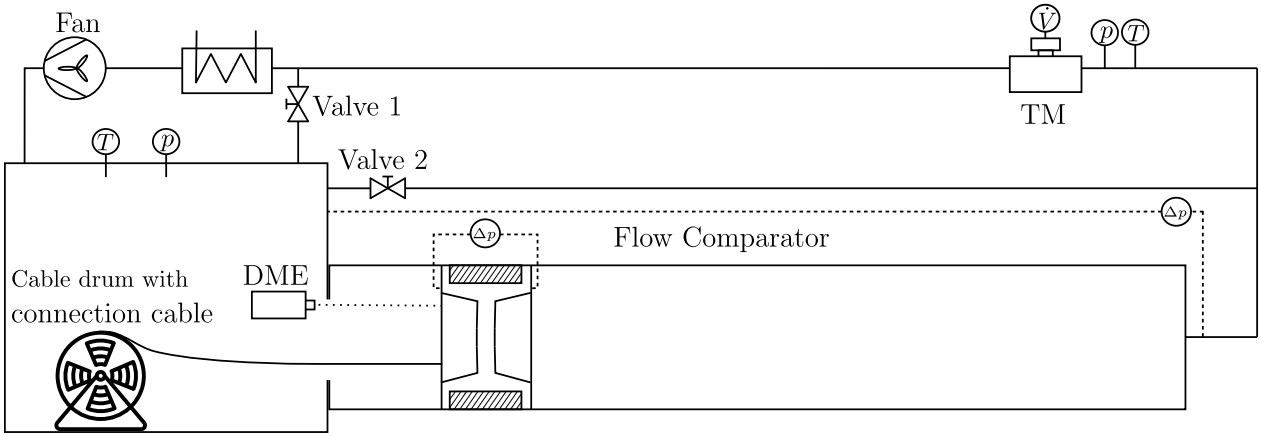


**Fig. 2.** Scheme of the experimental setup with the Flow Comparator in a closed-loop configuration.

The flow rate measurement and the calibration of the device under test (DUT) are based on the comparator principle [4]. Here, the DUT is a turbine meter (TM). The comparator principle compares the fluid properties upstream and downstream of the piston. In this case, the differential pressure and the difference in fluid velocity compared to the piston is used. Therefore, a sensor measures the differential pressure at the piston. Additionally, a flow sensor measures the fluid flowing through a specified leakage in the piston. The ambient temperature and pressure as well as the temperature and pressure at the turbine meter are measured. The position of the piston is measured using a distance measuring equipment (DME).

A fan is used to set the volume flow rate through the turbine meter. The bypass valve 1 is installed due to the limited fan control accuracy. It is used to control the set volume flow rate with higher accuracy.

At the beginning of the experiment, the volume flow rate is set by the fan and the opening of valve 1. Valve 2 is open and the flow is bypassing the cylinder to achieve stationary conditions in the loop. As soon as stationary conditions are obtained, the piston slowly moves upstream. When the piston reaches the beginning of the cylinder, Valve 2 is closed and the piston is accelerated downstream until the piston velocity is close to the fluid velocity. Due to the limited control accuracy of the linear induction motor, there will be a small difference in piston velocity and fluid velocity. This is taken into account using various correction methods. The measurement phase starts when the piston velocity is close to the fluid velocity. The volume flow rate indicated by the Flow Comparator $\dot{V}_{\mathrm{FC}}$ can be calculated as shown in Eq. (1).

$$\dot{V}_{\mathrm{FC}} = \frac{V_{\mathrm{FC}}}{\Delta t_{\mathrm{FC}}} \tag{1}$$

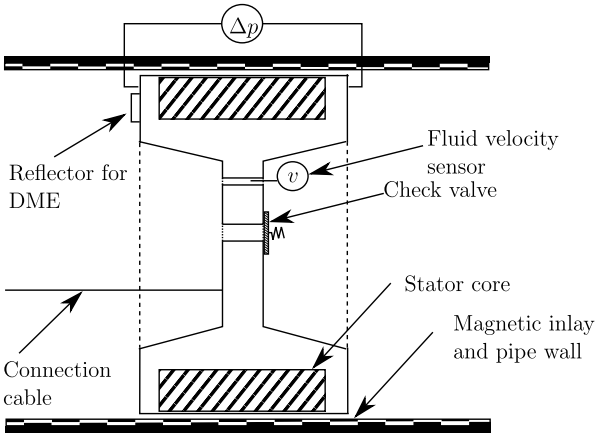


**Fig. 3.** Detailed scheme of the Flow Comparator piston as linear induction motor.

During the measurement phase, the discrete pulses of the turbine meter are counted. The volume flow rate indicated by the turbine meter can be calculated using the discrete pulses per time span and a proportionality factor known from previous calibration or from manufacturer specifications. The calibration's result is the relative deviation $f$ of the real volume flow rate to the indicated volume flow rate at a certain volume flow rate and pressure. The relative deviation $f$ is calculated as stated in Eq. (2).

$$f = \frac{\dot{V}^{\mathrm{c}}_{\mathrm{TM}} - \dot{V}^{\mathrm{c}}_{\mathrm{FC}}}{\dot{V}^{\mathrm{c}}_{\mathrm{FC}}} \cdot 100 \tag{2}$$

The Flow Comparator's calibration accuracy can be improved using a corrected volume flow rate indicated by the Flow Comparator $\dot{V}^{\mathrm{c}}_{\mathrm{FC}}$ instead of the above calculated volume flow rate $\dot{V}_{\mathrm{FC}}$. This can be achieved by applying correction methods based on the measured data of the integrated sensors in the piston. The correction of the turbine meter's volume flow rate is based on the characterization of the turbine meter with a first order differential equation describing the equilibrium of torque as presented in [5].

In the ideal scenario the piston velocity is the same as the fluid flow velocity for the entire measurement phase and the differential pressure and the velocity difference measured by the flow sensor piston would be zero. In the experiment, however, small differences of the piston velocity to the fluid velocity occur. The first correction method is based on the differential pressure across the piston. A non-zero differential pressure at the piston results into a leakage around the piston. A relationship between the differential pressure and the leakage can be derived by appropriate experiments and can be used to correct the volume displaced by the piston. The relationship is shown in Eq. (3) with the fitting parameters $a$ and $b$.

$$\dot{V}_{\mathrm{Leak},\Delta p} = a \cdot \Delta p + b \cdot \Delta p^2 \tag{3}$$

For small pressure differences, viscous leakage flow is assumed with transition to turbulent flow for increasing pressure difference. The correction method based on the differential pressure is practical for relatively high leakage flows. The integrated velocity sensor is used for smaller leakage flows. The relationship between the indicated velocity by the flow sensor and leakage flow is shown in Eq. (4).

$$\dot{V}_{\mathrm{Leak},v} = c v + d v^2 \tag{4}$$

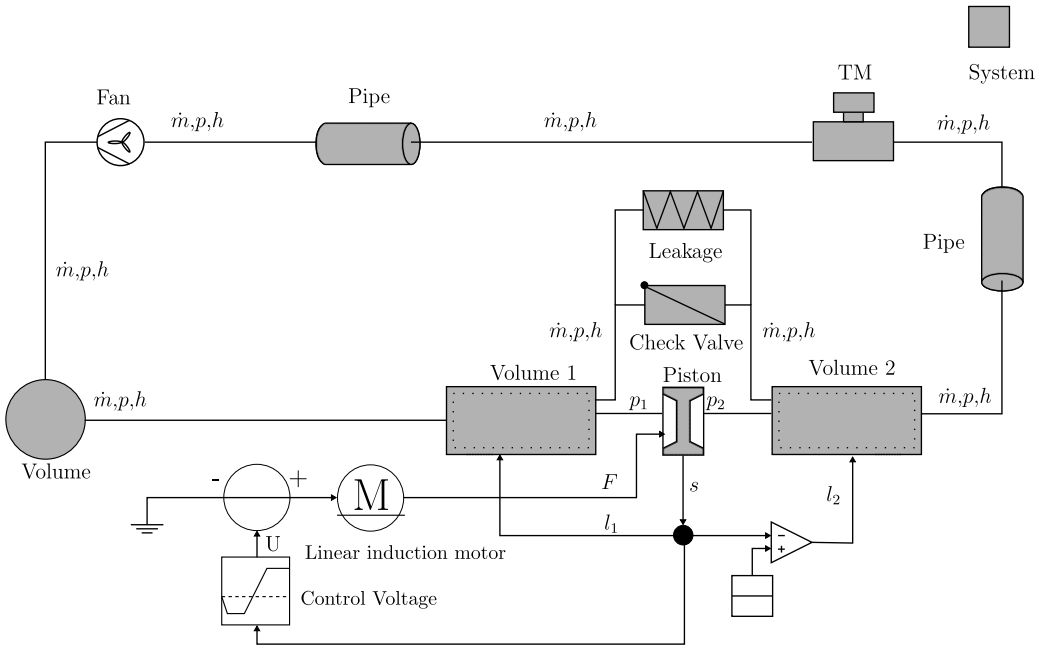


**Fig. 4.** Graphical representation of the computational model.

## 3. Modelica

Modelica® is an object-oriented, non-proprietary and equation-based language to conveniently model components of different physical domains which can be connected to model complex physical systems. The models are described by ordinary differential equations (ODE) in time, algebraic and discrete equations. The first specification for the Modelica language was released in 1997. It is developed by the non-profit Modelica Association. The Modelica Association is also responsible for the development of the open source Modelica Standard Library (MSL) which contains about 1600 model components and 1350 functions from different domains [6].

Several components of the MSL containing equations of different physical domains, e.g. fluid flow, thermodynamics, tribology and electrical engineering are used in the developed model to describe the Flow Comparator's dynamic behavior. The components are easily reusable due to the equation-based and object-oriented modeling approach. The media model used in the models can be easily exchanged allowing to test the model with atmospheric air as well as high pressure natural gas.

In addition, the equation-based modeling approach minimizes the chances of error due to equation conversion and increases the readability of the written code. The physical equations are transformed into a mathematical equation system. During the transformation, an optimizer improves the equation system e.g. a symbolic index reduction, alias elimination, etc. are executed. The optimized equation system is solved using numerical integration methods. Dymola® 2019 is used as simulation environment to develop and evaluate the Flow Comparator model in Modelica. The used solver is *dassl*, an implicit, higher order, multi-step solver with a step-size control. The used integration tolerance is $10^{-6}$.

## 4. Model description

A graphical representation of the developed model is shown in Fig. 4. The assumptions used in the model are [7]:

- pressure losses are proportional to the dynamic pressure,
- the gas flow is one dimensional,
- the system is adiabatic,
- potential energy of the gas is neglected,
- the heat transfer in the gas can be neglected in comparison to convective energy transport.

The model is an extension of the model presented in [8] and for simplicity purposes the bypass valve 2 is neglected in this approach.

All the boundary conditions as well as global parameters are set in the system model. Furthermore, it is possible to define the used fluid in the system model.

The Flow Comparator's measuring cylinder is modeled as one volume upstream of the piston (Volume 1) and one volume downstream of the piston (Volume 2). The enclosed gas volumes of the measuring pipe depend on the position of the piston and change with piston movement. In direction of the fluid flow a spatial discretization is applied to resolve the fluid flow in the measuring cylinder with higher accuracy. In order to achieve this, the finite volume method with the staggered grid approach is used. In a staggered grid, the scalar variables are located in the control volume center while the velocity and momentum variables are stored on the cell faces as shown in Fig. 5. The pressure loss due to friction $p_{\mathrm{f},i}$ is calculated using the detailed wall friction model from the MSL.

The measuring pipe volumes can store mass $m$, internal energy $m \cdot u$ and momentum $m \cdot v$ as described in Eqs. (5)–(7).

$$\frac{dm_i}{dt} = \dot{m}_i + \dot{m}_{i+1} \tag{5}$$

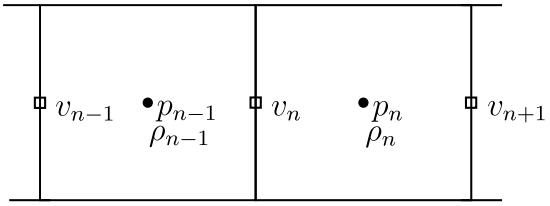


**Fig. 5.** Scheme of the staggered grid approach.

$$\frac{d}{dt}(mu)_i = \dot{m}_i\left(h_i + \frac{v_i^2}{2}\right) + \dot{m}_{i+1}\left(h_{i+1} + \frac{v_{i+1}^2}{2}\right) + \left(\frac{p_{i+1} - p_i + p_{f,i+1} - p_{f,i}}{2}\right)\dot{V}_i \tag{6}$$

$$\frac{d}{dt}(mv)_i = \dot{m}_i|v_i| + \dot{m}_{i+1}|v_{i+1}| - A\left(p_{i+1} - p_i\right) - A\left(p_{f,i+1} - p_{f,i}\right) \tag{7}$$

The piston's motion is determined using the equilibrium of forces at the piston as described by Eq. (8).

$$m_P \ddot{s}_P = p_1 A_P - p_2 A_P - F_{F,P} - F_{F,CC} + F_{LIM} \tag{8}$$

Pressure $p_1$ and $p_2$ are the pressures upstream and downstream right next to the piston, respectively. The friction force $F_{F,P}$ is calculated using a constant roll resistance coefficient $c_R$. The resistance due to the connection cable $F_{F,CC}$ depends on the position and is calculated using the connection cable's weight.

The piston's movement is controlled by the force induced by the linear induction motor $F_{LIM}$. The LIM is modeled using the space-vector equivalent circuit shown in Fig. 6. The main differences to the equivalent circuit of a rotatory induction motor are an eddy current resistance $R_r$ and a factor $f(Q)$ in the transversal branch. The differences occur due to the end effect phenomenon in a LIM which influences the magnetizing inductance and the eddy current resistance in the transversal branch. This is taken into account by the so-called end effect factor $Q$ which is defined in Eq. (9) [9].

$$Q = \frac{\tau_m R_r}{\left(L_m + L_{\sigma r}\right) v} \tag{9}$$

The end effects increase with the air-gap thickness (results in higher leakage inductance $L_{\sigma r}$) as well as with higher machine speed $v$ and reduce with increasing inductor length $\tau_m$[8]. The magnetizing inductance and the resistance vary with the term $f(Q)$:

$$f(Q) = \frac{1 - e^{-Q}}{Q} \tag{10}$$

The control voltage depends on the position of the piston and changes sign and value at the starting position. It has a specified stopping time $t_{stop}$ and a rising time $t_{rise}$. The frequency inverter uses the control voltage and a constant voltage to frequency characteristic to determine the voltage for the LIM.

The turbine meter model uses a constant pressure loss coefficient $\zeta_{TM}$ to describe the pressure loss occurring in the turbine meter. Furthermore, the model uses a relationship between indicated volume flow rate and real volume flow rate as described in [10].

The pipes are modeled using the DynamicPipe model of the MSL. The model uses balance equations for the mass $m$, the momentum $m \cdot v$ and the internal energy $m \cdot u$.

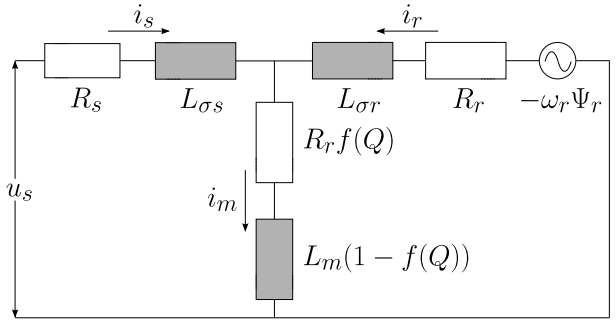


**Fig. 6.** Space-vector equivalent circuit of the LIM.

## 5. Validation

The Flow Comparator model's accuracy is highly relevant for the prediction of the closed-loop systems dynamic behavior and the components interaction. The model's accuracy is affected by the aforementioned general assumptions, the accuracy of the given LIM parameters, the assumptions for the friction force, and further simplifications.

Experiments are conducted as described in Section 2 and the measurement data is used for model validation. The model is only validated for the part of the experiment where the piston moves forward and the actual calibration of the meter under test is executed. For the experiment and the simulation, the same control voltage trajectory is used to validate the model of the LIM and the frequency inverter.

In Fig. 7, the measured and simulated piston velocity for three different control voltages is shown. During the measurement and simulation, the fan is turned off, resulting into no fluid flow produced by the fan. For all control voltages, the simulation has a slightly lower acceleration than the measurement during the starting phase. Furthermore, the control voltages 1.6 V and 2 V show an small oscillation during the measurement when reaching the maximum velocity. This dynamic behavior is not modeled as it occurs due to the random variations while unwinding connection cable. The unwinding of the connection cable is slightly different in each measurement depending on many factors e.g. starting position, volume flow rate, number of measurement run etc. After the piston accelerates to the velocity linked with the used control voltage, the simulation and measurement data have a similar value for all control voltages. Also, the decrease in piston velocity due to the connection cable's increasing resistance force shows a similar behavior in simulation and measurement.

The piston velocity as well as the differential pressure at the piston for a volume flow rate of $\dot{V} = 100\,m^3/h$ are shown in Fig. 8. The frequency inverter control voltage is set to achieve zero differential at the piston. The simulation is done with the same control voltage and overall a good accordance of measurement data and simulation is achieved. However, the differential pressure at the start of the measurement phase differs in measurement and simulation. This is due to the missing bypass in the simulation and therefore the differential pressure starts with a negative value. Furthermore, in the simulation the differential pressure at the piston increases a little more than in the measurement data. A similar behavior is observable for the piston velocity as it decreases slightly faster in the simulation than in the measurement.

## 6. Optimization

The model is used to optimize the control voltage trajectory of the frequency inverter to achieve maximum available measuring time with

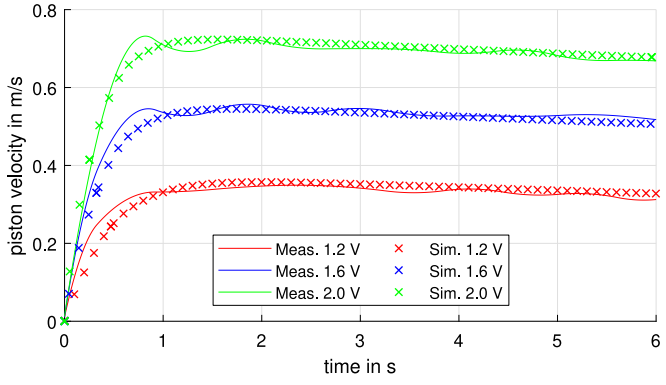


**Fig. 7.** Comparison of the piston velocity over the time in the model and measured data for different control voltages with turned off fan.

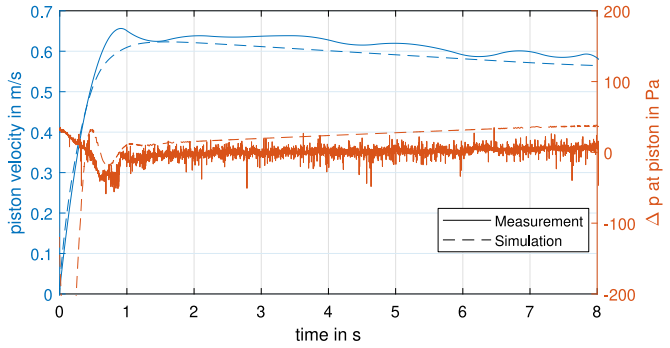


**Fig. 8.** Comparison of velocity and differential pressure at the piston for a volume flow rate of $\dot{V} = 100\,\mathrm{m^3/h}$ and a control voltage of 1.8 V.

zero differential pressure at the piston. In order to achieve this, the trajectory in Fig. 9 is applied to the model. It has an overshoot of control voltage at the beginning and an increasing slope during the measuring phase to offset the increase of connection cable resistance. This approach results into four optimization parameters to maximize the available measuring time:

- maximum control voltage $u_{max}$
- time at maximum control voltage $t_{max}$
- minimum control voltage $u_{min}$
- increasing control voltage slope $u_{rise}$

The optimization is conducted using MATLAB 2019a in combination with Dymola 2019. The optimization algorithm is run in MATLAB and the simulation of the Flow Comparator is done in Dymola using the parameters given by the optimization algorithm. This allows parallel simulation of several models with different parameter combinations and therefore a much faster optimization time.

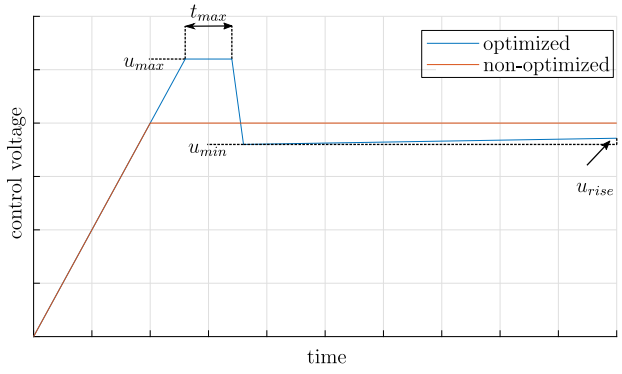


**Fig. 9.** Exemplary control voltage trajectories for non-optimized and optimized case.

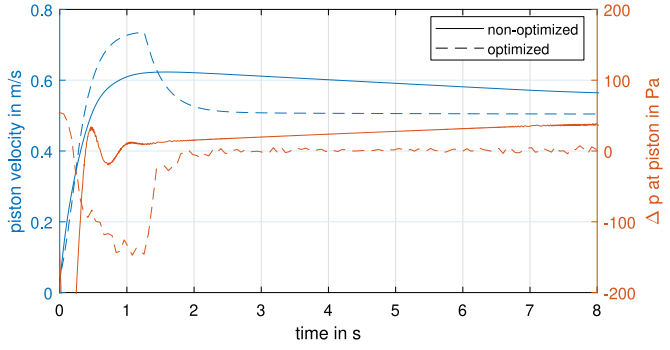


**Fig. 10.** Comparison of velocity and differential pressure at the piston for a volume flow rate of $\dot{V} = 100\,\mathrm{m^3/h}$ with optimized and non-optimized frequency inverter control voltage trajectory.

The simulation result for the optimized and non-optimized control voltage trajectory is shown in Fig. 10. The piston velocity is lower in the optimized case and remains at an almost constant value throughout the simulation. The overshoot in control voltage also appears in the piston velocity. Due to this, the differential pressure initially decreases more than in the non-optimized case. However, after the decrease the differential pressure in the optimized simulation decreases to zero and stays at that value for the remaining simulation.

## 7. Conclusion

The Flow Comparator in a closed loop configuration is modeled using the modeling language Modelica®. The implemented model is successfully validated against measurement data of the actual flow comparator prototype. A simple optimization of the control voltage trajectory to maximize the available measuring time is conducted as application example of the developed model. The result of optimization will allow to extend the upper limits of the flow rate usable for calibrations. Additionally, the possibility to gather detailed information about pressure and temperature development at arbitrarily chosen locations in the system with high time resolution enables much better and more reliable statements about the accuracy of the flow rate measurement with this system.

The linear induction motor model describes the electromechanical interaction. In future work, it will be essential to extend the model by heat transfer from the motor components to the gas to complete the modeling of the overall thermodynamic performance of the Flow Comparator.

Furthermore, the bypass needs to be considered in the model. This would allow the model to be used for actual predictions of the Flow Comparator's dynamic behavior in a loop configuration with the desired event sequence. Also, the friction force of the piston needs to be measured more accurately. This includes the position depending friction force, the velocity depending friction force as well as the increase of counter force due to the connection cable weight. Based on this, a more detailed optimization approach can be used to counteract small deviations which could affect an uniform piston velocity.

## Nomenclature

| | |
|---|---|
| Greek symbols | |
| $\Delta$ | difference |
| $\omega_r$ | electric frequency, rad $\mathrm{s^{-1}}$ |
| $\Psi_r$ | induced part flux, Wb |
| $\rho$ | density, kg $\mathrm{m^{-3}}$ |
| $\tau_m$ | polar pitch, m |
| $\zeta$ | pressure loss coefficient, dimensionless value |
| Latin symbols | |
| A | area, $\mathrm{m^2}$ |
| $a, b, c, d$ | fitting parameters, dimensionless value |
| $c_R$ | roll resistance coefficient, dimensionless value |
| $F$ | force, N |
| $f$ | relative deviation, % |
| $h$ | enthalpy, J $\mathrm{kg^{-1}}$ |
| $i$ | current, A |
| $L$ | inductance, H |
| $l$ | length, m |
| $m$ | mass, kg |
| $\dot{m}$ | mass flow rate, kg $\mathrm{s^{-1}}$ |
| $p$ | pressure, Pa |
| $Q$ | end effect factor, dimensionless value |
| $R$ | resistance, $\Omega$ |
| $s$ | position, m |

| | |
|---|---|
| $t$ | time, s |
| $u$ | internal energy, J $kg^{-1}$ |
| $u_s$ | voltage, V |
| $V$ | volume, $m^3$ |
| $v$ | velocity, m $s^{-1}$ |
| $\dot{V}$ | volume flow rate, $m^3h^{-1}$ |
| Subscripts, Superscripts and Abbreviations | |
| c | corrected |
| CC | Connection cable |
| DME | Distance measuring equipment |
| DUT | Device under test |
| FC | Flow Comparator |
| f | friction |
| HPPP | High pressure Piston Prover |
| i | index |
| Leak | Leakage |
| LIM | Linear induction motor |
| m | main |
| MSL | Modelica standard library |
| ODE | Ordinary differential equations |
| P | Piston |
| $\sigma$ | leakage inductance |
| r | Rotor |
| s | Stator |
| TM | Turbine meter |

## CRediT authorship contribution statement

**Sukhwinder Singh:** Conceptualization, Methodology, Software, Formal analysis, Validation, Visualization, Writing - original draft. **Gerhard Schmitz:** Supervision, Writing - review & editing. **Bodo Mickan:** Conceptualization, Software, Writing - review & editing.

## Declaration of competing interest

The authors declare that they have no known competing financial interests or personal relationships that could have appeared to influence the work reported in this paper.

## References

[1] G. Schmitz, A. Aschenbrenner, Experience with a Piston Prover as the New Primary Standard of the Federal Republic of Germany in High-Pressure Gas Metering, in: Proceedings of the 18th World Gas Conference, Berlin, 1990, 8.-12.7.1991.

[2] Physikalisch-Technische Bundesanstalt PTB, Prüfschein der Rohrprüfstrecke, 1991.

[3] Physikalisch-Technische Bundesanstalt PTB, PTB Mitteilungen, Special Issue 119 (1), 2009.

[4] B. Mickan, R. Kramer, Evaluation of two new volumetric primary standards for gas volume established by PTB, in: Proceedings of the 7th International Symposium on Fluid Flow Measurement (ISFFM), Anchorage, Alaska, August 12-14, 2009, 2009, http://www.measurementlibrary.com/docs_library/events/isffm2009/Docs/17.pdf.

[5] H.-B. Böckler, Messrichtigkeit von mechanischen Gasmessgeräten bei Verwendung von unterschiedlichen Gasbeschaffenheiten, Dissertation, Universität Duisburg-Essen, 2019.

[6] The Modelica Association, Modelica Language, Eingesehen am 22.11.2019, https://modelica.org/.

[7] M. von der Heyde, G. Schmitz, B. Mickan, Modeling of the german national standard for high pressure natural gas flow metering in modelica, in: Proceedings of the 11th International Modelica Conference, Versailles, France, September 21-23, 2015, Linköping University Electronic Press, 2015, http://dx.doi.org/10.3384/ecp15118663.

[8] S. Singh, G. Schmitz, B. Mickan, Modeling of the flow comparator prototype as new primary standard for high pressure natural gas flow metering, in: Proceedings of the 13th International Modelica Conference, Regensburg, Germany, March 4–6, 2019, in: Linköping Electronic Conference Proceedings, Linköing University Electronic Press, 2019, pp. 671–678, http://dx.doi.org/10.3384/ecp19157671.

[9] J.-H. Sung, K. Nam, A new approach to vector control for a linear induction motor considering end effects, in: Conference Record of the 1999 IEEE Industry Applications Conference. Thirty-Forth IAS Annual Meeting (Cat. No.99CH36370), IEEE, 1999, pp. 2284–2289, http://dx.doi.org/10.1109/IAS.1999.799162.

[10] B. Mickan, R. Kramer, V. Strunck, Transient response of turbine flow meters during the application at a high pressure piston prover, in: 15th Flow Measurement Conference (FLOMEKO), Linköping University Electronic Press, 2010.